SAE The Engineering Society
For Advancing Mobility
Land Sea Air and Space

# COMBUSTION, HEAT TRANSFER AND ANALYSIS

## P-182

ational Off-Highway & Powerplant
ress & Exposition
ukee, Wisconsin
mber 8-11, 1986

# COMBUSTION, HEAT TRANSFER AND ANALYSIS

## P-182



*The papers included in this volume are abstracted and indexed in the SAE Global Mobility Database*

SAE GLOBAL MOBILITY DATABASE

Published by:
Society of Automotive Engineers, Inc.
400 Commonwealth Drive
Warrendale, PA 15096
September 1986

860537PG

ISBN 0-89883-746-4
SAE/P-86/182
Library of Congress Catalog Card Number: 86-62212

# PREFACE

This Proceedings contains papers presented in the sessions "Combustion, Heat Transfer & Analysis" at the 1986 International Off-Highway and Powerplant Congress & Exposition. The word "International" is appropriate. Countries (nations) participating are: Sweden, Great Britain, India, Republic of China, Japan, People's Republic of China, and the United States of America.

Contained in this Proceedings are many topics suitable for research workers, engine designers, students, professors, and interested persons wishing to follow the latest developments.

A partial listing of topics broken down into three categories are listed below:

I. Engine designers

— cold starting
— effect of variable swirl
— effect of combustion chamber geometry
— effect of injection systems
— IDI dual throat jet swirl chamber
— two stage heat release

II. Research oriented

— use of high speed photography
— addition of oxygen
— method of measuring soot particles
— effect of fuel adhering on the cold wall
— simulation model for a dual fuel engine
— model of jet mixing in cross flow
— heat release tests using a bomb
— measuring piston temperature

III. "Adiabatic" related

— heat transfer into ceramic combustion chamber wall
— combustion phenomenon in adiabatic engines

A little philosphy: We feel presenting papers at a meeting is a two way street. The presenter wishes to have the technical world know what "he" is doing. The audience benefits by being exposed to the latest findings as well as to the discussions at the meeting, which they can use in their own laboratory or studies.

We, as co-organizers, wish to thank the authors and their sponsors for participating. We also wish to thank the behind-the-scene persons, the "screeners," who reviewed each paper for technical content and relayed their comments back to the authors. SAE staff is acknowledged for their cheerful help.

**Takashi Suzuki**
**Otto A. Uyehara**
Co-Organizers

# TABLE OF CONTENTS

861181

# Characterization of Combustion Processes in the Prechamber and Main Chamber of an Indirect Injection Diesel Engine by High-Speed Photography

**Keiya Nishida and Hiroyuki Hiroyasu**
University of Hiroshima

**Tsutomu Matsuoka and Hirobumi Yamauchi**
Mazda Technical Research Center

ABSTRACT

The combustion processes in the prechamber and the main chamber of a small indirect injection (I.D.I.) diesel engine were observed simultaneously by high-speed photography. These observations made it possible to characterize the behavior of flames in both chambers, that is, ignition of fuel, developing and rotating flames in the prechamber, and a flame jet spouting into the main chamber. The effect of engine variables, such as fuel injection timing, cross-sectional area of a throat, fuel injector location, and a recess in a piston top, on the combustion process as well as the engine performance were considered. A flame jet spouting into the main chamber separated into two directions and induced two vortexes. Brown sooty flames appeared along the prechamber wall and inside the flame jet which struck on the piston top. The higher-velocity flame jet and the two intense vortexes induced by the flame jet realized superior fuel consumption and lower smoke emission.

IN AN INDIRECT INJECTION (I.D.I.) DIESEL ENGINE, a combustion chamber is divided into a prechamber and a main chamber which are connected to each other by a throat. Gas motion and combustion in both chambers proceed, being related to each other through the throat. Thus, the correlation between the phenomena in both chambers must be investigated in order to comprehend the characteristics of I.D.I. diesel engine combustion, which often differ from those of a direct injection (D.I.) diesel engine. In the present study, the combustion processes in the prechamber and the main chamber of the small I.D.I. diesel engine were observed simultaneously by high-speed photography. These two combustion sequences made it possible to analyze the correlation between the combustion processes in both chambers. A transparent piston engine with a cylinder head incorporating a transparent window provided the main chamber and the prechamber with optical access from the under and lateral sides of both combustion chambers respectively. The modification for such optical access was made so as to maintain the original three-dimensional shapes of the combustion chambers, especially the prechamber, as much as possible. Most of the previous high-speed photographic studies (1-5) have been conducted on I.D.I diesel combustion in a two-dimensional prechamber, which is far from an actual shape. In addition, the correlation between combustion processes in the prechamber and the main chamber has been treated in few studies (1). The present study also discusses the effects of engine variables, such as fuel injection timing, cross-sectional area of the throat, fuel injector location and a recess in the piston top, on the combustion processes and the engine performance.

EXPERIMENTAL APPARATUS AND PROCEDURES

Figure 1 shows a transparent piston and prechamber engine with an optical arrangement used in this study. The basic engine was an in-line type, four-cylinder, I.D.I. diesel engine with a bore of 88.9 mm and a stroke of 89.0 mm. Main specifications of the engine combustion system are shown in Table 1. This engine has been modified a little for laboratory use, and a flat piston was mainly used in the main chamber instead of a recessed piston. For the combustion photography, the first cylinder of the engine was modified to provide the prechamber [3] with optical access from the lateral side of the cylinder head [1], and the main chamber [6] with optical access from the underside of the elongated piston [8]. The details of the combustion chambers in the transparent piston and prechamber engine are shown in Fig. 2. The prechamber had a slant bottom and a hemispherical dome whose design was based on the Ricardo Comet-V Swirl chamber. A Pyrex glass window was

*Numbers in parentheses designate references at end of paper.

attached to one side of the prechamber so as to maintain the original shape as much as possible. The transparent piston crown [14] (Fig. 1) in the main chamber was made of acrylic resin. Figure 3 shows the visual field of the high-speed camera. The visual field was 85 % of the prechamber cross-sectional area, and 65 % of the main chamber (cylinder) cross-sectional area at TDC. The throat exit in the main chamber could be observed within the visual field. When high-speed combustion photographs were taken, the engine was driven by an electric motor at 1000 rpm, and then operated with a fuel injection quantity of 33 mg/cycle. Since the compression ratio of this engine decreases to 17.5 compared with the basic unmodified engine, intake air and the prechamber wall were heated up to the temperature of 180°C and 200°C respectively in order to get the same ignition delay as that of the basic engine. The fuel used was diesel fuel. Both combustion chambers and the crank-angle mark on the flywheel circumferential surface were lighted by a xenon lamp [16]. The

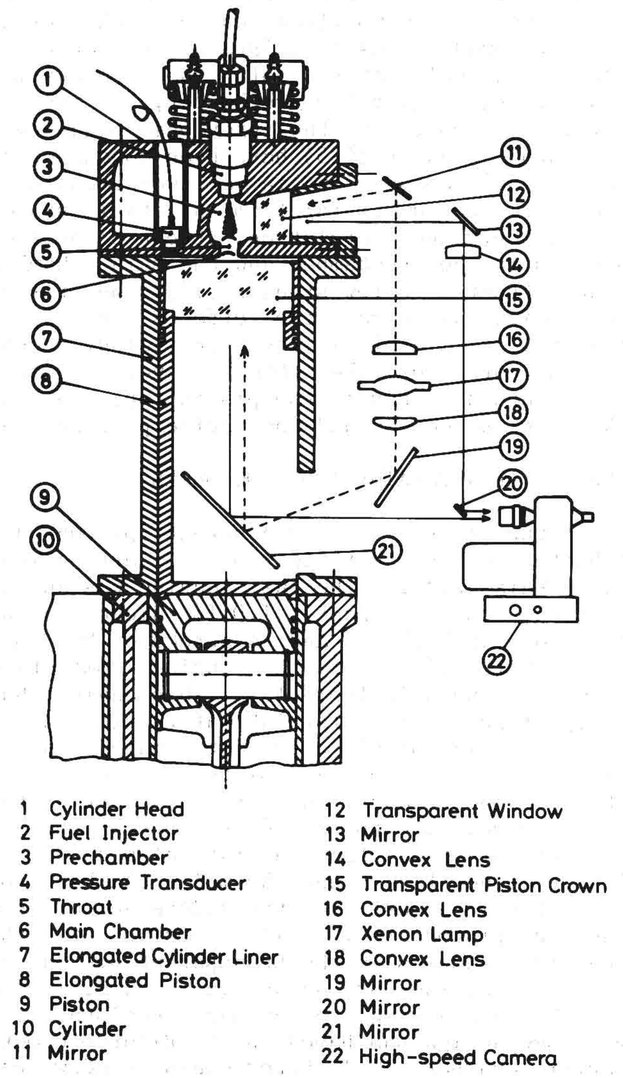


Fig. 1 - Transparent Piston and Prechamber Engine with Optical Arrangement

Table 1 - Engine Specifications

| | |
|---|---|
| Prechamber Type | Swirl Chamber |
| Main Chamber | Flat Piston |
| Bore | 88.9 mm |
| Stroke | 89.0 mm |
| Swept Volume | 0.552 L |
| Compression Ratio | 21.2 |
| Volume Ratio of Prechamber | 53.0 % |
| Injection Pump | Bosch - VE |
| Plunger Diameter | 9.0 mm |
| Injection Nozzle | Throttling - Pintle (DNOSD) |
| Valve Opening Pressure | 13.2 MPa |

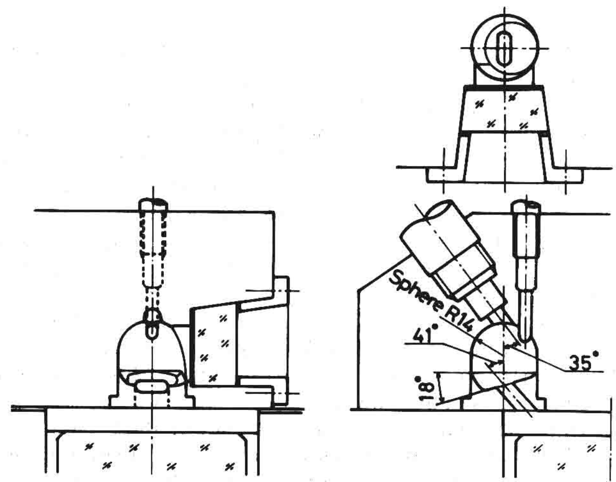


Fig. 2 - Details of Combustion Chamber

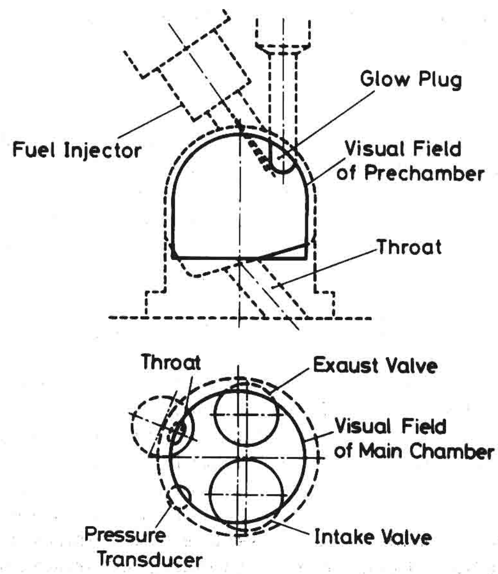


Fig. 3 - Visual Field

image of the prechamber was magnified about two diameters. The combustion photographs of the prechamber and the main chamber and the crank-angle mark were taken with a high-speed camera [21] at a film speed of about 8000 frames per second. At the same time, the pressure signal for the main chamber measured with a piezo-electric pressure transducer [4], a needle-lift signal from a fuel injector [2] and a crank-angle signal were stored in a data recorder. Since the engine showed almost stable running after three cycles from the start of fuel injection, the combustion sequences and the pressure diagrams were analyzed after the three firing cycles. Besides taking combustion photographs, a performance test of the basic engine was also carried out on output power and exhaust emissions, such as smoke, nitric oxides and unburned total hydrocarbons.

## EXPERIMENTAL CONDITIONS

Fuel injection timing, the cross-sectional area of the throat, the location of the fuel injector, and a recess in a piston top were chosen as experimental parameters, and they were varied as shown in Table 2. No.1 was adopted as a standard condition in this study. The fuel injection timing was changed from -2°CA to -7°CA and -12°CA after TDC(No.2 and No.3). The ratio of throat area $R_{th}$ meant the ratio of the cross-sectional area of a throat to that of the cylinder, and was changed from 1.2 % to 0.6 % and 2.4 % (No.4 and No.5), as shown in Fig. 4. The fuel injector location was changed from (A) to (B) and (C) (No.6 and No.7), as shown in Fig. 5. (A) is the standard location, where the injector was aimed at the glow plug, and the fuel spray was injected downstream into the swirling flow. In the case of (B), the fuel spray was injected toward the center of the prechamber, and perpendicular to the swirling flow near the nozzle. In the case of (C), the fuel spray was injected toward the entrance of the throat, and in the opposite direction of the swirling flow. The flat piston was finally changed to the recessed piston, in the shape of a Ricardo Comet-V main chamber, as shown in Fig. 6 (No.8).

Table 2 - Experimental Conditions

| No. | Injection Timing $\theta_{inj}$ | Ratio of Throat Area $R_{th}$ | Location of Fuel Injector | Main Chamber (Piston Top) |
|---|---|---|---|---|
| 1 | -2 °CA | 1.2 % | A | Flat |
| 2 | -7 | 1.2 | A | Flat |
| 3 | -12 | 1.2 | A | Flat |
| 4 | -2 | 0.6 | A | Flat |
| 5 | -2 | 2.4 | A | Flat |
| 6 | -2 | 1.2 | B | Flat |
| 7 | -2 | 1.2 | C | Flat |
| 8 | -2 | 1.2 | A | Recessed |

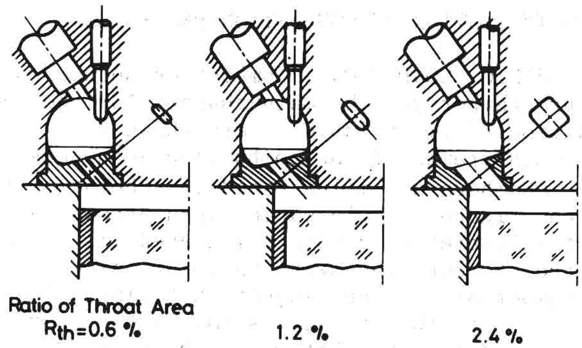


Fig. 4 - Shapes of Throat

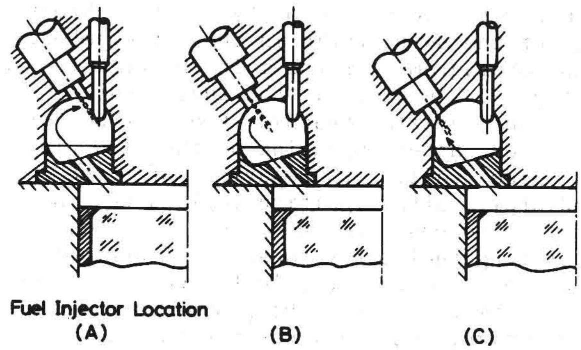


Fig. 5 - Injector Locations

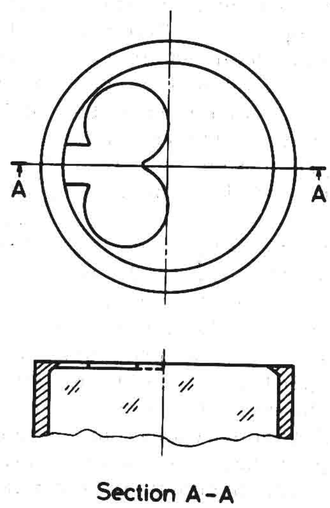


Fig. 6 - Shape of Piston Recess

## CHARACTERIZATION OF COMBUSTION PROCESSES

BASIC CONDITION - Combustion sequences of the prechamber and the main chamber for the basic condition (No.1 in Table 2) are shown in Fig. 7, and main frames of the combustion sequences for both chambers are illustrated in schematic form in the figure. Closed and open arrows in the first illustration denote calculated air velocity at the throat and swirl ratio of air in the prechamber at the fuel injection timing. The air velocity at the throat was calculated assuming pressure difference between both chambers to be neglected. The swirl ratio, defined as the ratio of rotating speed of air in the prechamber to engine revoling speed, was calculated based on the moment of momentum into the prechamber(6), and the prechamber was assumed to have a spherical shape with a radius of 14 mm. Calculated results for the basic condition was 8.9 m/s of the air velocity at the throat and 35.2 of the swirl ratio in the prechamber. The pressure diagrams for the main chamber are shown in Fig. 9. In Fig. 7, the fuel spray injected from the nozzle reached the bottom of the prechamber after impinging on the glow plug and the side wall. Behavior of the flame immediately after ignition implied the air-fuel mixing process to be as follows. The evaporating fuel spray passed the entrance of the throat and reached the left-side wall opposite the glow plug. Since the piston was descending at this time, the fuel was not spread by the air flow through the throat. The fuel stagnated at the bottom-left side and the vaporized fuel was distributed to the top side of the prechamber along the left-side wall by the swirl. Ignition occurrd at the bottom-left side and the flame extended initially along the wall where the vaporized fuel was distributed, next to the center of the prechamber and finally to the injecting fuel spray. The first flame in the main chamber was observed at this time. This flame seemed to be caused by the ignition of the fuel which had been drawn from the prechamber, or by flame propagation through this fuel from the flame in the prechamber. At 15°CA after TDC when flame propagation through the fuel in the main chamber almost finished, characteristic behavior of a flame jet, that is, a breathing was observed at the throat. In that moment, the flame was not found at the exit of the throat in the main chamber. Then the flame jet began to spout intensly and the pressure in the main chamber rose rapidly. The flame which extended over the prechamber showed a swirling motion, which included three-dimensional components and was more complex than a solid-body rotation. Swirl ratio in the prechamber estimated from the flame motiom was about 20 to 25 at 20°CA after TDC, and the swirl motion attenuated rapidly during the expansion stroke. The flame jet penetrating along the piston top separated into two directions and induced two vortexes. Then the flame jet reached the cylinder-liner wall opposite the throat. Brown sooty flames were seen along the wall of the prechamber and inside the flame jet impinging on the piston top.

EFFECT OF INJECTION TIMING - Figure 8 shows combustion sequences and schematic illustrations of the characteristic frames when the injection timing was changed from -2°CA (basic condition, No.1 in Table 2) to -7°CA and -12°CA after TDC (No.2 and No.3). Pressure diagrams for the main chamber and engine peformance for such injection timings are shown in Fig. 9 and 10 respectively. As seen from Fig. 10, brake mean effective pressure (BMEP) was slightly higher at the injection timing of -7°CA, and total unburned hydrocarbon (HC) emission was minimum at the same injection timing. As the injection timing was advanced, nitric oxides ($NO_x$) and smoke emissions increased.

The tendencies of $NO_x$ and smoke emissions to increase with the advance of fuel injection timing were explined from the combustion sequences as follows. As seen from the combustion sequences in Figs. 7 and 8, the flame in the prechamber developed more rapidly after the ignition owing to longer ignition delay and wider fuel distribution as the injection timing was advanced. Such a change of flame development in the prechamber implied that earlier fuel injection induced more intensive premixed combustion which caused higher $NO_x$ emission. Combustion period in the prechamber was lengthend and much more flame remained in the prechamber at 50°CA after TDC, when the injection timing was advanced. Earlier fuel injection reduced the amount of fuel drawn from the prechamber into the main chamber before ignition since the period from TDC to the end of injection, during which the air in the prechamber flowed into the main chamber, decreased. Thus, the amount of fuel which burned in the prechamber increased, and more unutilized air remained in the main chamber. Such process seemed to cause imperfect combustion, where much soot was generated. Moreover, the piston top at the beginning of flame-spouting into the main chamber came closer to the cylinder head as the injection timing was advanced. Thus, more of the flame jet into the main chamber impinged on the piston top immediately after the beginning of spouting, and the amount of fuel in the flame jet, which was quenched on the wall and prevented from mixing with air, increased. Such a flame jet seemed to contain much soot.

After the flame extended over the prechamber, it showed almost the same motion in both the chambers under any injection timing. The flame in both chambers disappeared at 100°CA for any injection timing investigated.

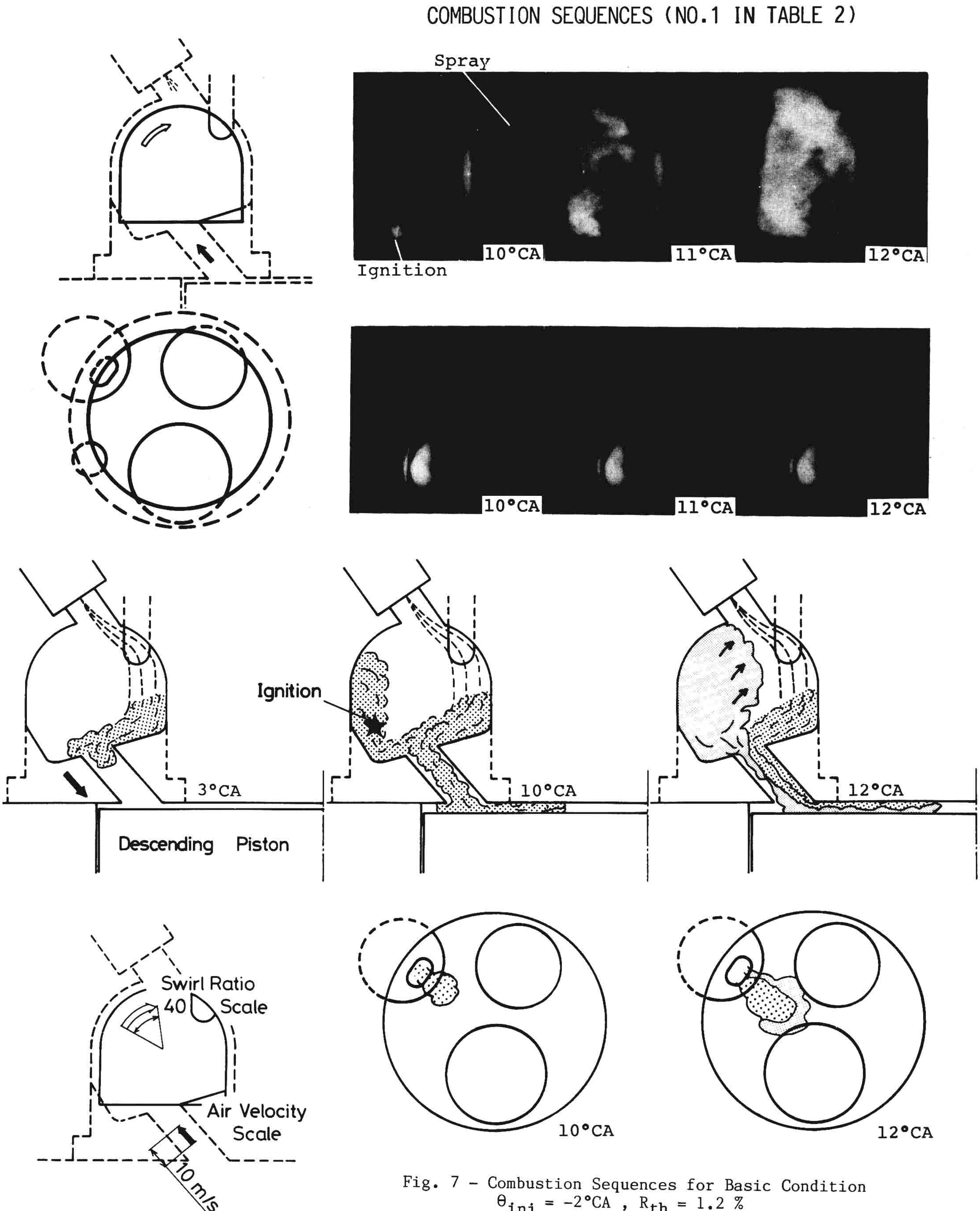


Fig. 7 - Combustion Sequences for Basic Condition
$\theta_{inj}$ = -2°CA , $R_{th}$ = 1.2 %
Injector Location : A , Flat Piston

COMBUSTION SEQUENCES (NO.1 IN TABLE 2, CONTINUED)

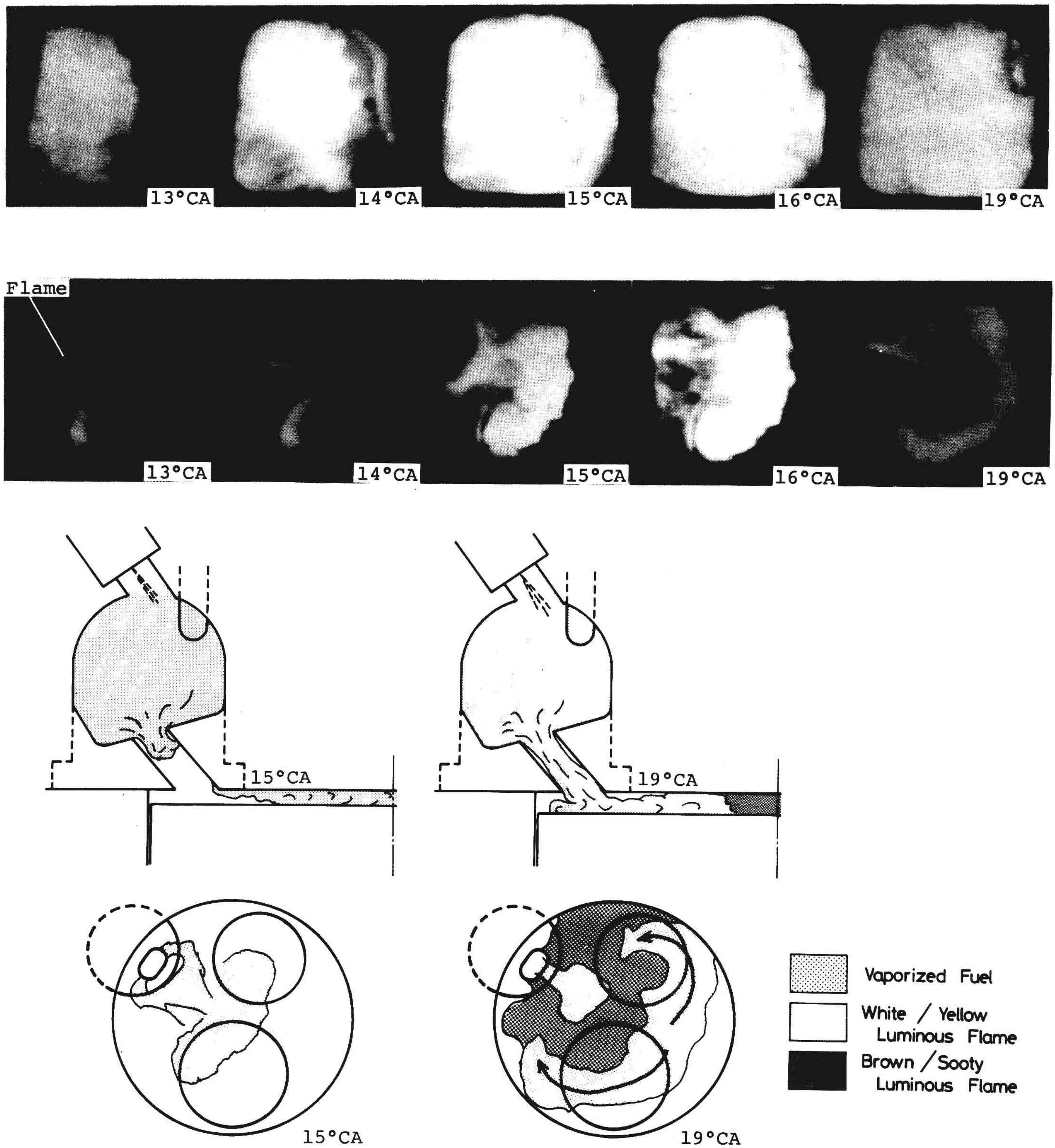


Fig. 7 - Combustion Sequences
for Basic Condition (Continued)

COMBUSTION SEQUENCES (NO.1 IN TABLE 2, CONTINUED)

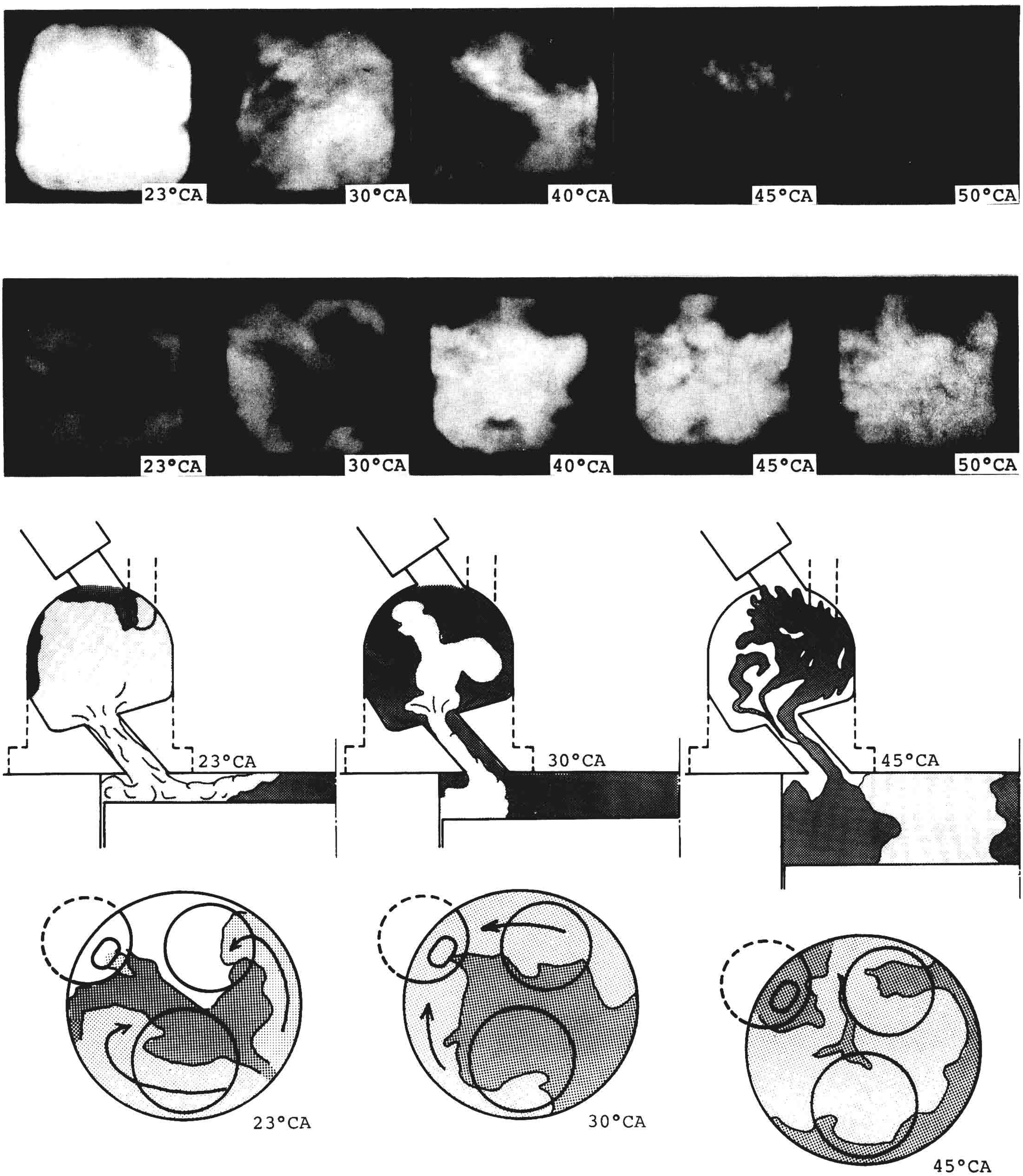


Fig. 7 - Combustion Sequences
for Basic Condition (Continued)

COMBUSTION SEQUENCES (NO.2 IN TABLE 2)

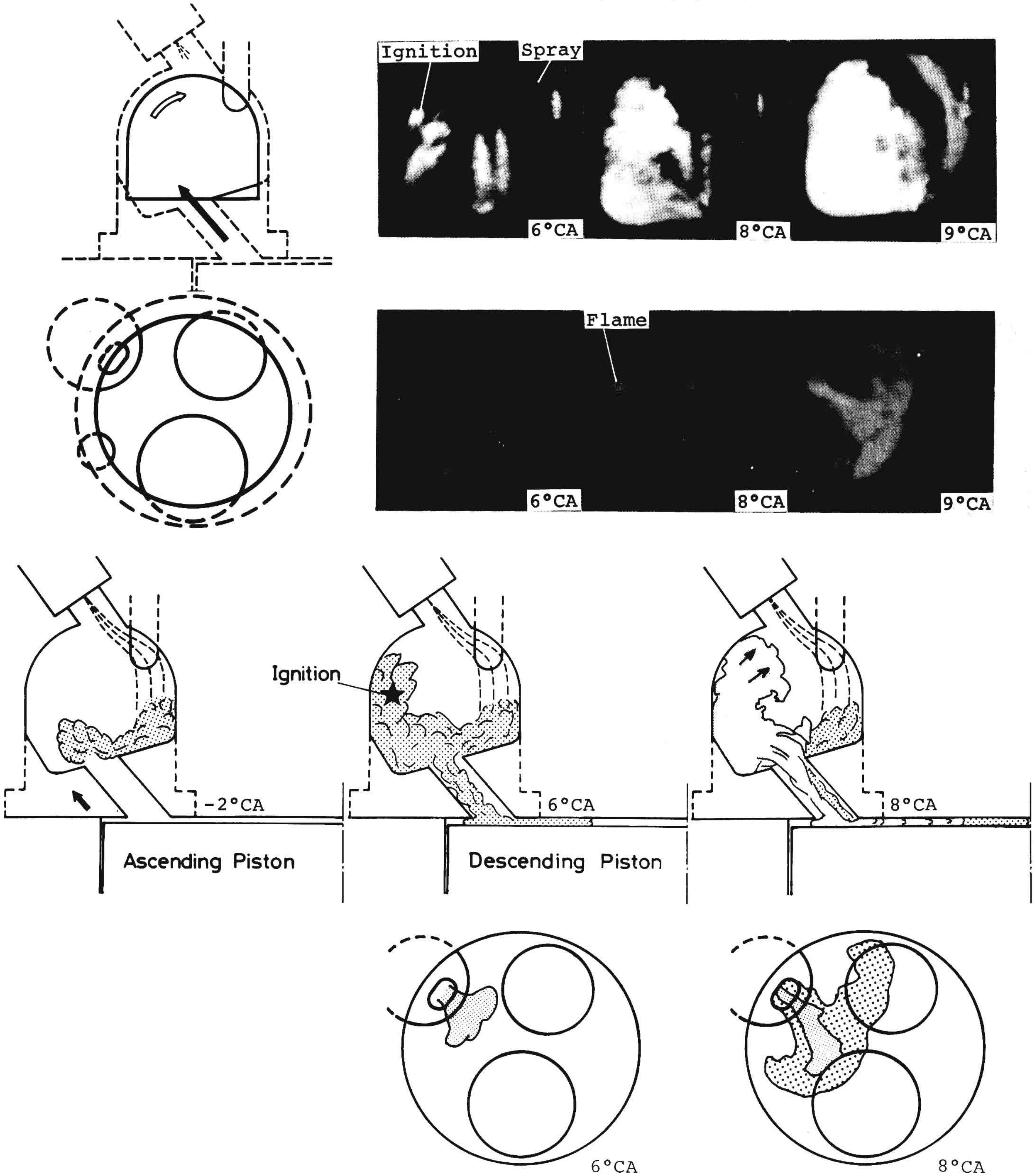


Fig. 8 (1) - Combustion Sequences for Injection Timing of -7°CA

COMBUSTION SEQUENCES (NO.2 IN TABLE 2, CONTINUED)

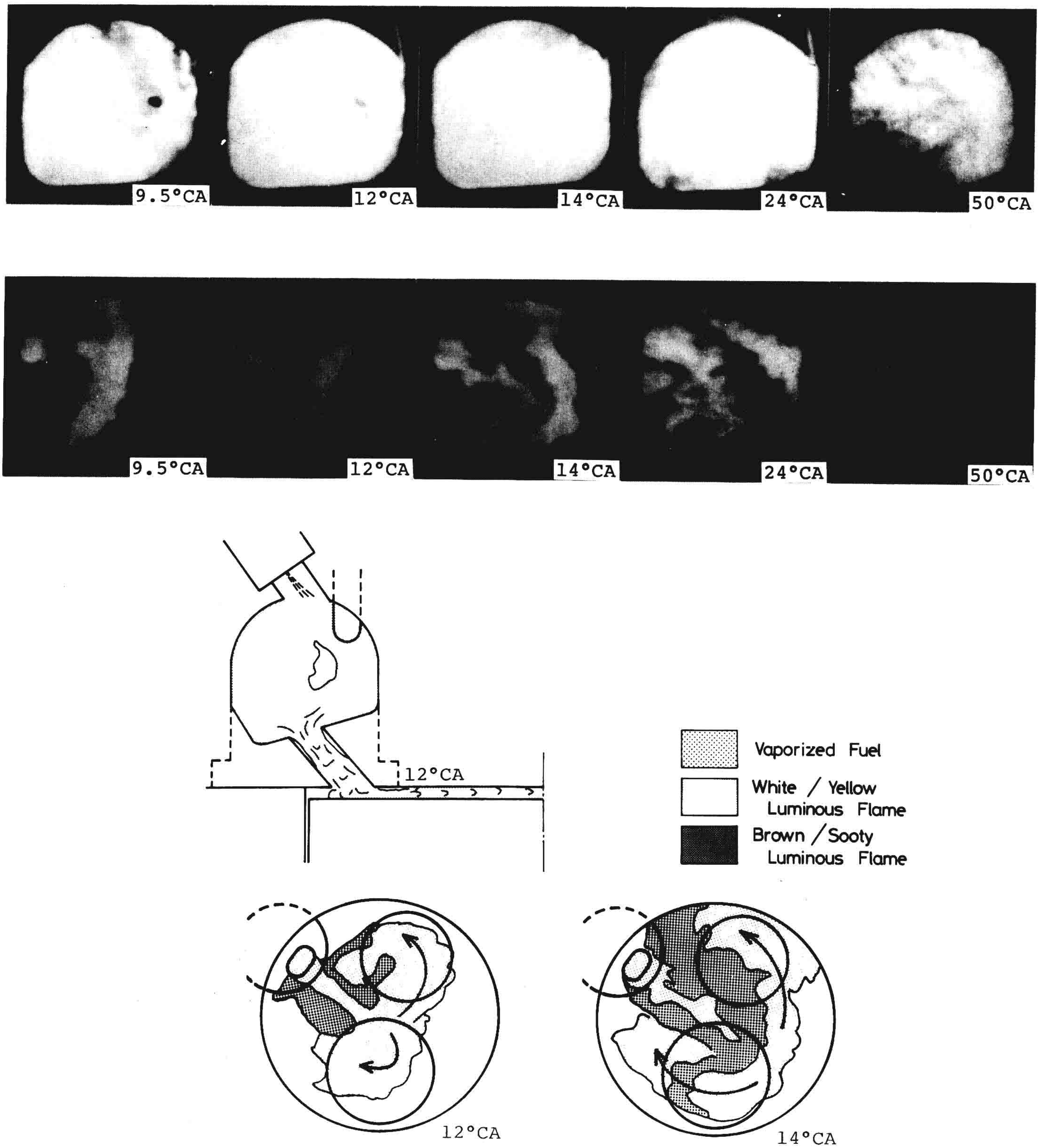


Fig. 8 (1) - Combustion Sequences for Injection Timing of -7°CA (Continued)

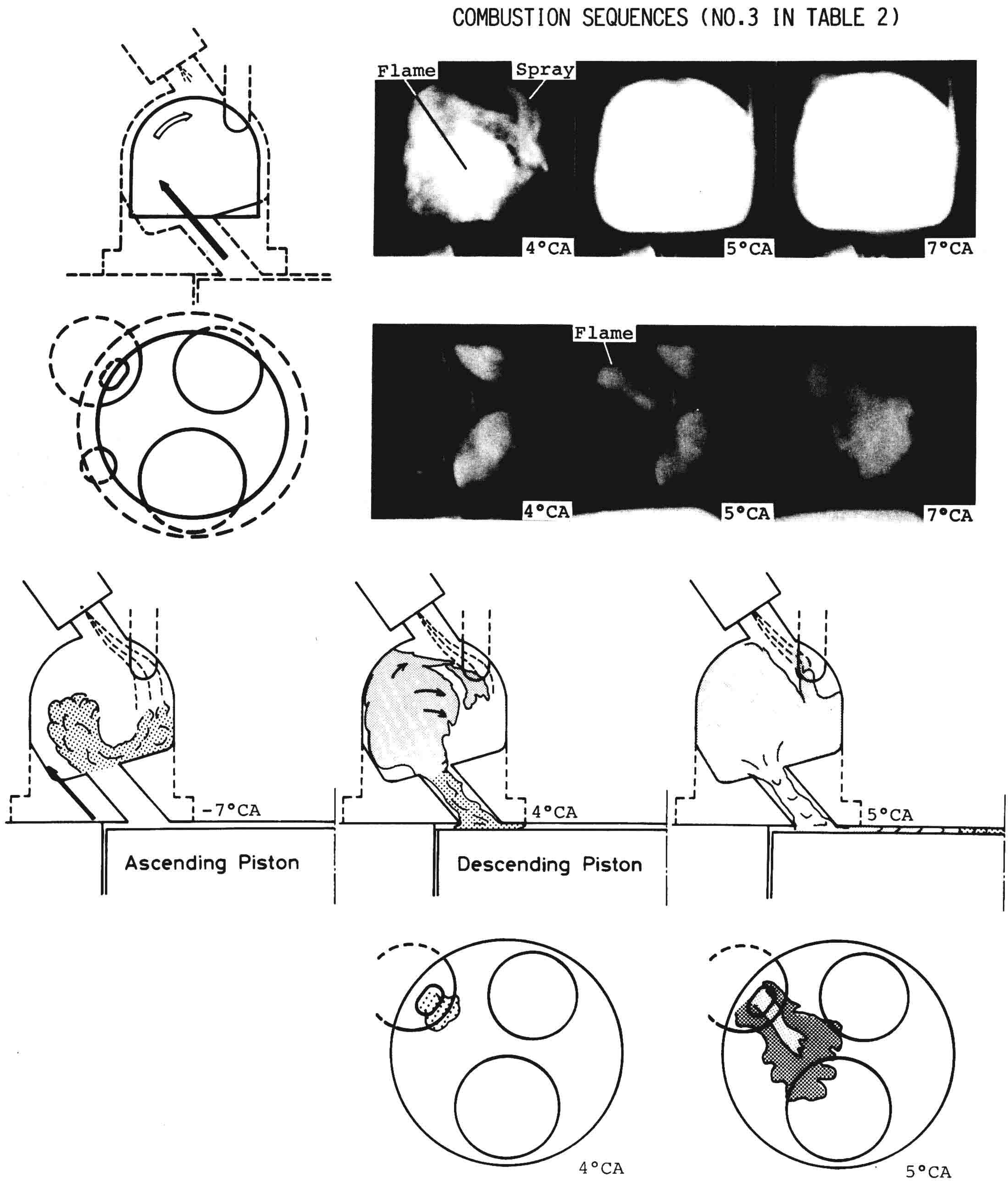


Fig. 8 (2) - Combustion Sequences for Injection Timing of -12°CA